Coupling Kinetic Modeling with Artificial Neural Networks to Predict the Kinetic Parameters of Pine Needle Pyrolysis

Langui Xu,[a] Lin Zhang,[a] Xiangjun He,[a] Wenbin He,[b] Ziyong Wang,[c] Weihua Niu,[d] Dong Wei,[d] Yi Ran,[e] Wendan Wu,[f] Mingjun Cheng,[f] Jundou Liu,[g] and Ruyi Huang [a,e,*]

The pyrolysis behavior of biomass is critical for industrial process design, yet the complexity of pyrolysis models makes this task challenging. This paper introduces an innovative hybrid model to quantify the pyrolysis potential of pine needles, predicting the entire process of their pyrolysis behavior. Through experimental analyses and kinetic parameter calculations of pine needle pyrolysis, the study employs a kinetic model with a chemical reaction mechanism. Additionally, it introduces an improved dung beetle optimization algorithm to accurately capture the primary trends in pine needle pyrolysis. The developed artificial neural network model incorporates meta-heuristic algorithms to address process error factors. Validation is based on experimental data from TG at three different heating rates. The results demonstrate that the hybrid model exhibits strong predictive performance compared to the standalone model, with coefficients of determination (R^2) of 0.9999 and 0.999 for predicting the conversion degree and conversion rate of untrained data, respectively. Additionally, the standard errors of prediction (SEP) are 0.249% and 0.449% for predicting the conversion degree and conversion rate of untrained data, respectively.

DOI: 10.15376/biores.19.4.7513-7529

Keywords: Pine needle pyrolysis; Kinetic model; Artificial neural networks; Prediction

Contact information: a: School of Mechanical Engineering, North China University of Water Resources and Electric Power, Zhengzhou 450011, China; b: School of Mechanical Engineering, Zhengzhou University of Light Industry, Zhengzhou, China; c: Henan ALST New Energy Technology Co. LTD, Zhengzhou 450001, China; d: Zhengzhou Yuzhong Energy Co., LTD, Zhengzhou, China; e: Biogas Institute of Ministry of Agriculture and Rural Affairs, Key Laboratory of Development and Application of Rural Renewable Energy, Ministry of Agriculture and Rural Affairs, Chengdu 610041, China; f: Sichuan Pratacultural Technology Research and Extension Center Chengdu 610041, China; g: Sichuan Agricultural Planning and Construction Service Center, Chengdu 610041, China;
**Corresponding author: huangruyi1983@qq.com*

INTRODUCTION

Biomass is globally acknowledged as a "zero carbon" renewable energy source (Huang *et al*. 2021), and its pyrolysis products hold vast potential for green economy applications, including biofuels and chemicals. Pyrolysis plays a crucial role in the formation and evolution of biomass fuels during the combustion process, exerting a direct impact on subsequent processes. Therefore, studying the pyrolytic properties of biomass is crucial for enhancing energy use efficiency (Gbolahan *et al*. 2022; Ke *et al*. 2022; Zhong *et al*. 2023). Due to the increasing demand for biomass fuels in science and industry, the study of the laws governing the pyrolysis and combustion behaviour of biomass is key to

the effective use of biomass fuels (Ragauskas *et al*. 2006; Zhu *et al*. 2021; Vo *et al*. 2022). The main components of biomass are hemicellulose, cellulose, and lignin; based on such a composition, chemical kinetics provides a theoretical basis for the quantitative description of pyrolysis reaction processes (Kersten *et al*. 2005; Ka *et al*. 2012; Ding *et al*. 2020; Ding *et al*. 2023). Biomass pyrolysis kinetics are used to characterize the effects of parameters such as reaction temperature and reaction time on the conversion of reaction products during thermal decomposition reactions of biomass (Xu *et al*. 2020). Many scholars have conducted extensive research on the kinetic parameters of biomass pyrolysis processes (White *et al*. 2011), providing important data for the design of pyrolysis reactors and subsequent combustion equipment. While the prediction results of the kinetic model agree to some extent with the experimental data, there are still significant discrepancies between them (Ding *et al*. 2019; Liborio *et al*. 2024). Machine learning models show exceptional accuracy in predicting highly non-linear processes and can automatically learn from data without the need for real operating and chemical conditions, greatly reducing the need for human intervention (Breiman 1996; Sunphorka *et al*. 2017; Naqvi *et al.* 2018; Hu *et al*. 2022). These models have been used extensively to simulate thermal processes involving biomass pyrolysis, gasification, and combustion (Dubdub and Al-Yaari 2020; Bi *et al*. 2021; Yang *et al*. 2022). However, machine learning models have certain drawbacks: Machine learning models typically depend on significant amounts of high-quality data. Insufficient data or poor data quality can negatively affect model performance. Many machine learning algorithms are described as black-box models, meaning that their inner workings are complicated and difficult to elucidate, making it challenging to understand and characterize the model's predictions (Dubdub and Al-Yaari 2020; Bi *et al*. 2021). In addition, machine learning models can accurately predict outcomes within the training domain, but they often perform poorly in domains outside the training data (Xing *et al*. 2019; Zhang *et al*. 2022). For example, forty-nine tobacco samples were used to study pyrolysis kinetics through machine learning approaches (Wei *et al.* 2023). A comprehensive artificial intelligence model without considering the chemical reaction mechanism was presented to predictive the thermal decomposition of rice husk (Alaba *et al.* 2019). A large amount of laboratory data poses significant challenges to predictive work. Moreover, non-mechanistic models lack interpretability and are highly dependent on data.

To enhance predictive capability, an innovative framework has been developed to improve the generalization of predictive models. In the framework, kinetic models based on chemical reaction mechanisms were integrated with data-driven machine learning models. Kinetic models based on chemical reaction mechanisms were used to predict optimize initial values of the kinetic parameters (Kaczor *et al*. 2020; Dubdub and AlYaari 2021; Marchese *et al*. 2024). The BP-ANN model was used to predict the error distribution of the kinetic parameters. A combination of kinetic and artificial neural network models was used to provide a comprehensive prediction of pyrolysis in the training and non-training zones.

Pine needles are abundant in resins and oils, known for their high calorific value, flammability, low ash content, and minimal emissions of nitrogen and sulfur pollutants, making them an effective biomass fuel source (Martín-Lara *et al*. 2016). In this study, pine needles were chosen as the research subject to explore a method that combines chemical kinetics-based models with data-driven models for predicting the pyrolysis process. The objectives of this study were to (1) Conduct pyrolysis experiments to investigate the relationship between pine needle conversion degree and temperature at various heating rates (10, 20, and 40 K/min). (2) Optimize the kinetic parameters of three components

using a kinetic model integrated with the mantis algorithm, and analyze the errors. (3) Utilize a BP-ANN model in conjunction with a genetic algorithm to predict errors in kinetic parameters and compare them with parameters obtained from a standalone kinetic model.

EXPERIMENTAL

Thermal Analysis Experiments

Pine needles were selected as samples for thermogravimetric (TG) experiments. The samples were initially ground in a grinder, and the resulting particles were then sieved through an 80-mesh sieve to achieve uniform particle size. The samples were baked at 423 K to ensure the evaporation of free and bound water (Zha *et al*. 2022). The pyrolysis process was conducted using a TA instruments (SDT Q600 Thermal Analyzer). Samples weighing 9.0 ± 0.5 mg were placed in an aluminum crucible and heated from 298 to 1173 K at heating rates of 10, 20, or 40 K/min. Nitrogen was circulated at a rate of 100 mL/min to maintain an ambient gas environment during pyrolysis.

Parallel Reaction Kinetic Modelling Predictions

The concept of kinetic parallel reaction prediction aims to optimize kinetic parameters using a kinetic model combined with an improved dung beetle optimization algorithm with TG experimental data. The method aims to predict the pyrolysis process of pine needles by utilizing optimized parameters and comparing experimental results with predicted outcomes to derive prediction deviations.

Kinetic modelling of parallel reactions

The decomposition of pine needles is considered as the sum of parallel reactions of three components: hemicellulose, cellulose and lignin (Machmudah *et al*. 2020). The parallel kinetics scheme for the three components is given as Eq. 1,

$$component_i \rightarrow (v_i)volatiles + (1 - v_i)char \quad (1)$$

where v_i represents the volatile yield of each component reaction. According to the Arrhenius equation, it is assumed that the reaction mechanisms of each component are all of one order. The reaction rates of these three components can be expressed as Eq. 2,

$$\frac{d\alpha_i}{dT} = \frac{A_i}{\beta} e^{-\frac{E_i}{RT}}(1 - \alpha_i) \quad i = 1 \sim 3 \quad (2)$$

where $\alpha_i = \frac{m_{i0} - m_i}{m_{i0} - m_{i\infty}}$ denotes the degree of response of the i-th component. The conversion degree (a) can be defined as follows,

$$\alpha = \frac{m_0 - m}{m_0 - m_\infty} \quad (3)$$

where m_0 and m_∞ represent the initial and final sample masses, respectively.

The total conversion degree is defined as the sum of individual component conversions and was calculated as follows,

$$\alpha = \frac{\sum_i r_i(m_{i0} - m_i)}{m_{i0} - m_{i\infty}} = \sum_i r_i \alpha_i \quad (4)$$

where r_i represents the initial mass fraction of component i, and $\sum_i r_i = 1$, the overall kinetic equation for the three-component can be expressed as Eq. 5,

$$\frac{\mathrm{d}\alpha}{\mathrm{d}T} = \sum_{\mathrm{i}} r_{\mathrm{i}} \frac{A_{\mathrm{i}}}{\beta} \mathrm{e}^{-\frac{E_{\mathrm{i}}}{\mathrm{RT}}} (1 - \alpha_{\mathrm{i}}) \quad \mathrm{i} = 1 \sim 3 \tag{5}$$

In Eq. 5, eight unknown parameters must be determined to fit the experimental data. The objective of the optimization method is to minimize the difference between the experimental and simulated values. This is achieved by minimizing the sum of the squared differences between the experimental and simulated mass loss values at all heating rates, as shown in Eq. 6,

$$S_{DTG} = \sum_j S_j = \sum_j \sum_k [(\frac{d\alpha}{dT})_{j,k}^{exp} - (\frac{d\alpha}{dT})_{j,k}^{simu}]^2 + \sum_j \sum_k [(\alpha)_{j,k}^{exp} - (\alpha)_{j,k}^{simu}]^2 \tag{6}$$

here the superscripts "exp" and "simu" represent the experimental and simulated values, respectively. The index "j" represents the number of heating rates, and "k" represents the number of data points in the experiment. In optimization computations, the parameters R^2 and SEP were used to assess the discrepancy between experimental and simulated values.

Improved Dung Beetle Optimization Algorithm

The Dung Beetle Optimization Algorithm (DBO) is a mathematical model inspired by the behavior of dung beetles, including rolling balls, dancing, foraging, stealing, and breeding. The algorithm performs an iterative update through the following steps: initializing the dung beetle population, evaluating the fitness of individual dung beetles, updating the position and orientation of the dung beetles, and finally outputting the optimal solution (Xue and Shen 2022; Zhu *et al*. 2024). However, the dung beetle optimization algorithm has limitations in global search and tends to converge slowly when dealing with complex optimization problems. Therefore, this study proposes an improved dung beetle optimization algorithm (Shen *et al*. 2023). The improved dung beetle optimization algorithm enhanced the convergence speed and accuracy of the search process by introducing an initialized logistic chaos mapping population and improving the position update mechanism of individuals in the population using the Sinusoidal Algorithm (MSA). In addition, an adaptive Gauss-Cauchy perturbation modification strategy was used to enhance the adaptability and robustness of the model for complex problems. Compared to the traditional dung beetle algorithm, the MSADBO algorithm demonstrates a significant improvement in search efficiency and solution quality (Guo *et al*. 2023).

Artificial Neural Network (ANN) Model Predictions

The deviations predicted by the kinetic model based on chemical reactions were used as training inputs for the neural network. A genetic algorithm was then introduced to construct a data-driven back-propagation neural network model to predict the errors calculated by the kinetic model.

Back propagating artificial neutral net (BP-ANN) model

BP-ANN, a multilayer neural network using an error backpropagation algorithm, is renowned for its powerful learning and nonlinear mapping capabilities, making it one of The BP-ANN consists of an input layer, hidden layers, and an output layer, where information is transferred between neurons across different layers. The number of neurons in the input and output layers is determined by the input parameters and output targets, respectively, while the number of neurons in the hidden layer can be adjusted as needed (Cheng *et al*. 2022).

GA-BP-ANN Collaboration Model

Genetic algorithms (GA) are widely used in artificial neural networks due to their robustness, stochastic nature, global perspective, and inherent parallel processing capabilities (Quan *et al*. 2016). The main objective of integrating genetic algorithms with artificial neural networks is to use genetic algorithms to optimize the weighting parameters of artificial neural networks, replacing traditional, inefficient, and less intelligent learning algorithms with more effective advanced methods based on genetic algorithms (Conn *et al*. 1991). The backpropagation mechanism in BP-ANN searches for the extrema of a nonlinear function using the gradient method, which can lead to the issue of getting trapped in local minima. In contrast, GA possesses a powerful macro search capability and demonstrates excellent global optimization performance. They continuously enhance the quality of candidate solutions by simulating natural selection and genetic variation processes, thereby approaching closer to the global optimal solution. Therefore, this study combined GA with BP-ANN to leverage their complementary strengths, effectively overcoming the local extremum problem inherent in the backpropagation algorithm. This integration improved the overall performance and accuracy of the neural network (Zhu *et al*. 2020).

Coupled Kinetic Model and GA-BP-ANN Model Predictions

The kinetic model, enhanced by the dung beetle optimization algorithm, predicted the kinetic parameters of each component. These optimal parameters were then utilized to predict the pyrolysis of pine needles. The model predictions were compared with experimental (TG) data to calculate differences. These differences served as input data for training the GA-BP-ANN model to predict the error values generated by the kinetic model. The prediction results from the kinetic model were combined with the error predictions from the GA-BP-ANN model to generate the overall prediction data. Figure 1 illustrates the framework of this integrated approach.

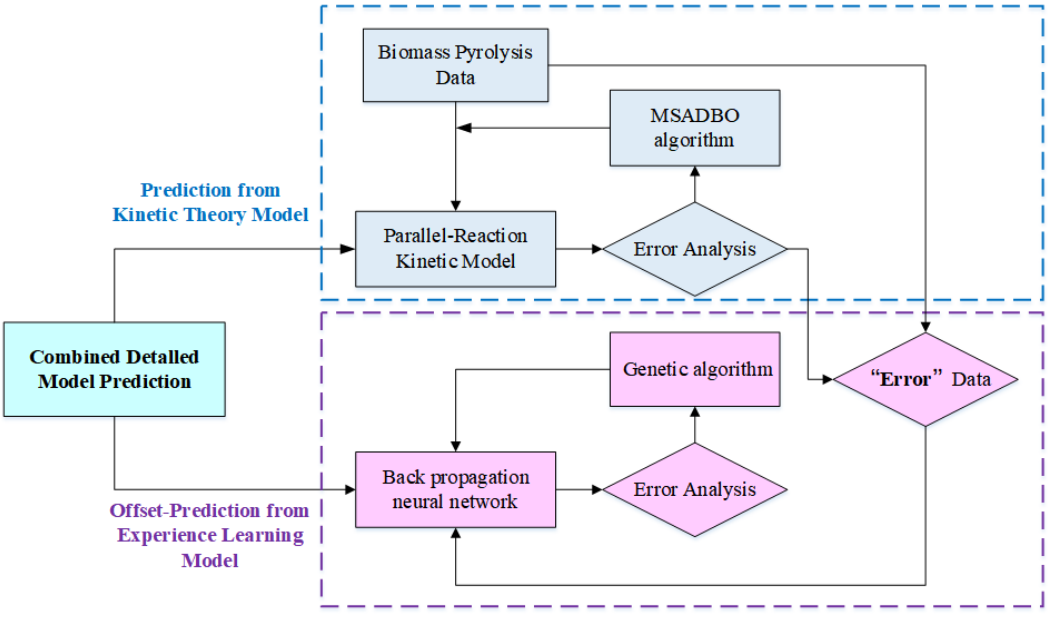

Fig. 1. Structure of coupled schematic diagram of the GA-BP-ANN

RESULTS AND DISCUSSION

Thermogravimetric Analysis

Figure 2 displays the conversion degree (α) and conversion rate ($\mathrm{d}\alpha/\mathrm{d}T$) curves for three heating rates. The pyrolysis process of pine needles occurred between 420 K and 800 K, with a peak occurring between 600 K and 650 K. Additionally, distinct shoulder regions appeared on either side of the peak. As the heating rate increased, both the shoulder and the peak shifted to higher temperatures, which is consistent with Chang *et al*. (2008). The increasing prominence of the shoulder region indicates an increase in the complexity of the reaction, implying the presence of multiple overlapping reactions. This complexity makes it challenging to construct an accurate kinetic model to predict pyrolysis behavior.

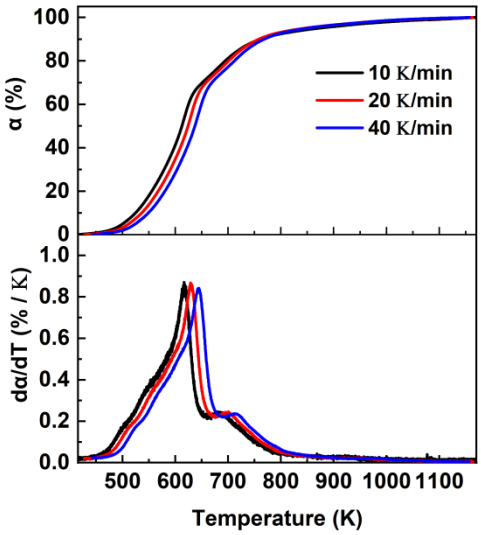

Fig. 2. Curves of conversion degree ($\boldsymbol{\alpha}$) and conversion rate ($\frac{\mathbf{d}\boldsymbol{\alpha}}{\mathbf{d}\boldsymbol{T}}$) at three heating rates

Kinetic Modelling Predictions

In this study, a kinetic model and the MSADBO algorithm were introduced to predict the kinetic parameters of hemicellulose, cellulose and lignin from TG data. The optimized initial values of the kinetic parameters (A and E_a) for hemicellulose, cellulose, and lignin were calculated using the iso-conversion method of the Kissinger-Kai method (Xu *et al*. 2023), as shown in Table 1.

Table 1. Optimal Parameters by MSADBO on Two Heating Rates

Substances	Parameters	Initial values	Search Range	MSADBO	
				Optimized Values	Difference of paramaters
Hemicellulose	E_1 (KJ/mol)	162.08	122-202	155.08	4.32%
	$\ln A_1[\ln(s^{-1})]$	34.78	26-38	29.71	14.58%
	r_1	0.38	0.28-0.48	0.48	26.32%
cellulose	E_2 (KJ/mol)	165.46	125-205	107.46	35.05%
	$\ln A_2[\ln(s^{-1})]$	31.46	24-36	32.93	4.67%
	r_2	0.26	0.16-0.36	0.36	38.46%
lignin	E_3(KJ/mol)	184.33	144-224	177.33	3.80%
	$\ln A_3[\ln(s^{-1})]$	31.67	24-36	30.01	5.24%
	r_3	0.36	0.16-0.56	0.16	4.32%

The parameters of the pine needle pyrolysis model to be optimized consisted of three aspects (9 parameters in total): the initial mass fraction (r_i) and the chemical kinetic parameters (A_i, E_i) for hemicellulose, cellulose, and lignin. Since the sum of the mass fractions of the three main components is 1, only eight parameters need to be optimized. Table 1 shows the initial values and search ranges for these optimization parameters. Note that the optimization process did not include TG data at a heating rate of 40 K/min. The optimal kinetic parameters derived from the optimization were then used to predict the biomass conversion degree (α) and conversion rate ($d\alpha/dT$), in the trained regions (10 and 20 K/min) and the untrained region (40 K/min), as shown in Fig. 3.

In Fig. 3 (a-c), the model's trend in predicting the conversion degree at the three heating rates was generally accurate, but there were some notable differences, mainly from 400 to 600 K, and 650 to 900 K. In Fig. 3 (d-f), the model predictions for the conversion rate showed significant errors in the shoulder regions on both sides of the peak, corresponding to the error regions in the conversion degree. These results indicate that the prediction model needed improvement and should be the focus of future research.

Table 2 shows that the R^2 values for the kinetic modeling of conversion degree were all above 0.98, while the predicted R^2 values for conversion rate were all below 0.75. Additionally, the standard error of prediction (SEP) for conversion degree and conversion rate in untrained zones were 3.570% and 9.409%, respectively. Although the model performed well in predicting conversion, it still needs to be improved in predicting the conversion rate. This suggests that further optimization and refinement are needed for the prediction model to improve its overall predictive performance.

Table 2. R^2 and SEP from the Kinetic Model

Heating Rate (K/min)	Conversion Degree (α)		Conversion Rate ($\frac{d\alpha}{dT}$)	
	R^2	SEP (%)	R^2	SEP (%)
10	0.9898	4.049	0.7217	9.543
20	0.9905	3.569	0.7455	9.405
40	0.9905	3.570	0.7412	9.409

GA-BP-ANN Model Predictions

The GA-BP-ANN model was trained using experimental data collected at heating rates of 10 and 20 K/min. The trained model was used to predict the conversion degree (α) and the conversion rate ($d\alpha/dT$) at the trained heating rates (10 and 20 K/min), as well as at an untrained heating rate (40 K/min). Figure 4 compares the experimental values with the predicted values at three heating rates.

In Fig. 4 (a-f), the predictions for the conversion degree (α) and conversion rate ($d\alpha/dT$) in the training temperature ranges (10 and 20 K/min) were in general agreement with the experimental data. However, around the peak temperature (about 630 K) for all three heating rates, there was a noticeable underestimation and leftward shift between the predicted and experimental values of $d\alpha/dT$, particularly evident in the untrained range. This observation is supported by the R^2 and SEP values in Table 3: within the trained range, the R^2 values for predicted conversion degree (α) were all above 0.995 and for $d\alpha/dT$ they were all above 0.97. Conversely, in the untrained range (40 K/min), the R^2 value dropped to 0.994, and for $d\alpha/dT$ it dropped to approximately 0.95.

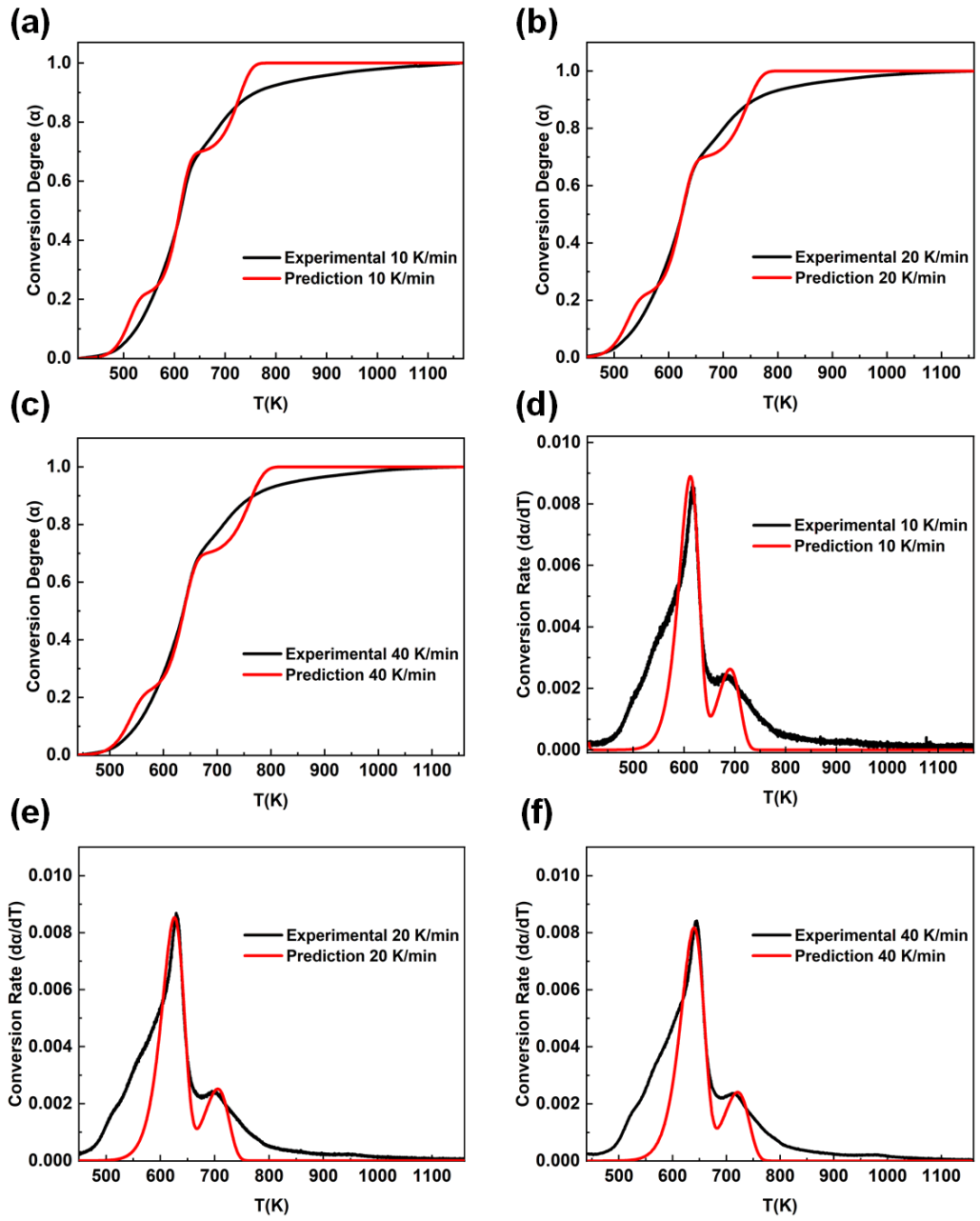

Fig. 3 (a-f). α and $\frac{d\alpha}{dT}$ predictions from the Kinetic Model

Compared to the traditional dynamics prediction model, the GA-BP-ANN model showed significant advantages with significantly lower SEP values and higher prediction accuracy. Specifically, the SEP value of the conversion degree in the training region was only 0.554% and 0.508%, and the SEP value of the conversion rate was 2.323% and 2.171%. This result indicates that the GA-BP-ANN model was able to fit the training data well and provide relatively accurate predictions. However, when the model was applied to untrained regions, there was a significant drop in prediction performance. In these untrained regions, the SEP value for the degree of conversion increased to 0.774%, while the SEP value for the conversion rate increased to 4.615%. This change indicates that although the GA-BP-ANN model performed well in the trained regions, its predictive

ability was relatively weak in the untrained regions. Overall, as a data-driven approach, the GA-BP-ANN model demonstrated excellent performance within the training domain but exhibited significant deterioration in performance outside the trained conditions, highlighting the model's limitations in extrapolating to untrained scenarios.

Table 3. R^2 and SEP from the GA-BP-ANN Model

Heating Rate (K/min)	Conversion Degree (α)		Conversion Rate ($\frac{d\alpha}{dT}$)	
	R^2	SEP (%)	R^2	SEP (%)
10	0.9955	0.554	0.9756	2.323
20	0.9971	0.508	0.9763	2.171
40	0.9948	0.774	0.9508	4.615

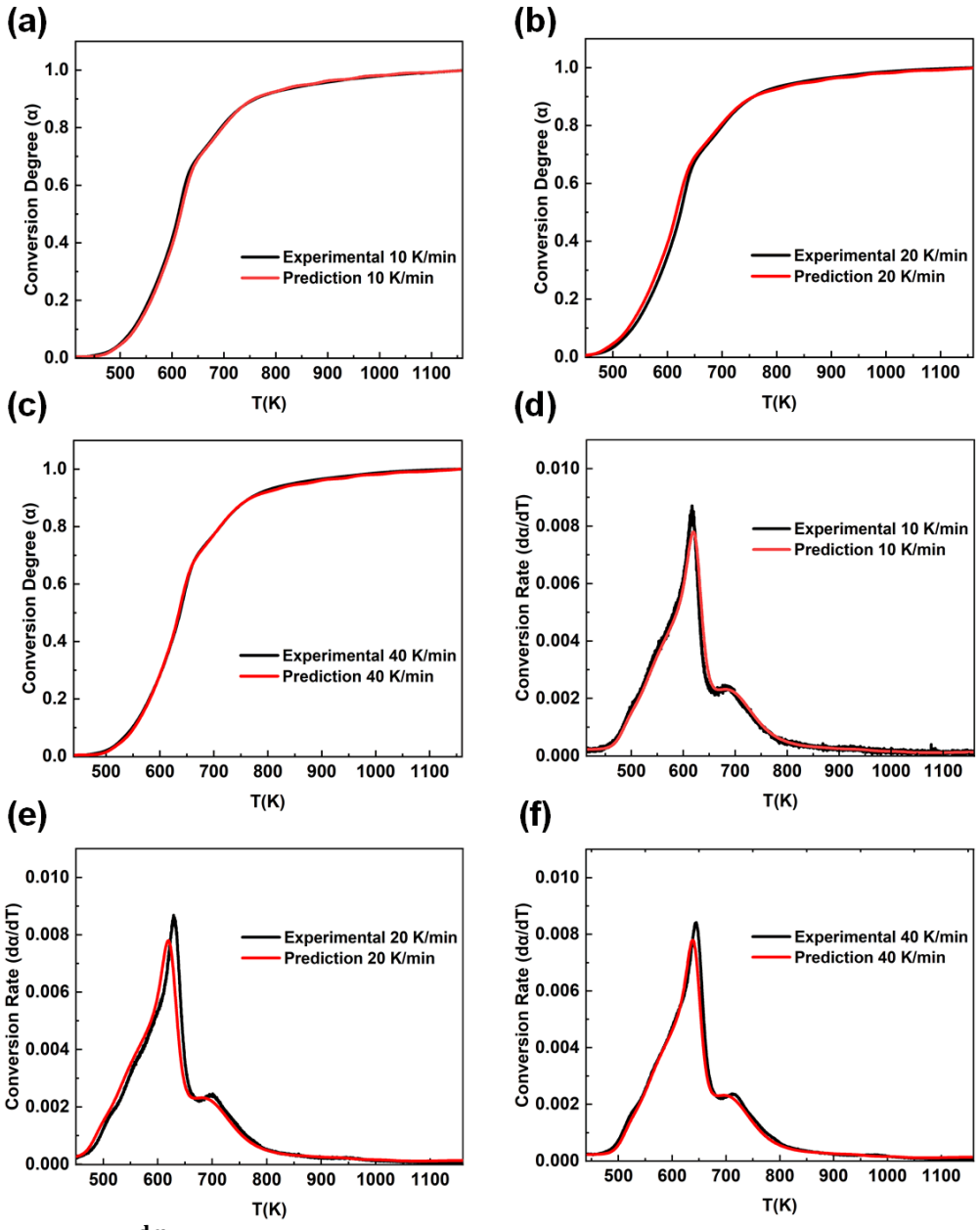

Fig. 4 (a-f). α and $\frac{d\alpha}{dT}$ predictions from the GA-BP-ANN Model

Kinetic-ANN Coupled Model Predictions

A kinetic model was used to predict the main trends in pyrolysis, and a GA-BP-ANN model was used to predict process deviations. Together, these two parts made the complete prediction. Figure 5 parts (a-f) depict the complete predictions of conversion degree (α) and conversion rate ($d\alpha/dT$) by the coupled model for heating rates of 10, 20 (trained region) and 40 K/min (untrained region). These figures show that the predictions of the coupled model closely matched the experimental data. The coupled kinetic-ANN model exhibited significant improvement over separate models, particularly in regions not explicitly trained. This indicates that coupled models were more effective in capturing and predicting trends in experimental data, especially when dealing with complex datasets.

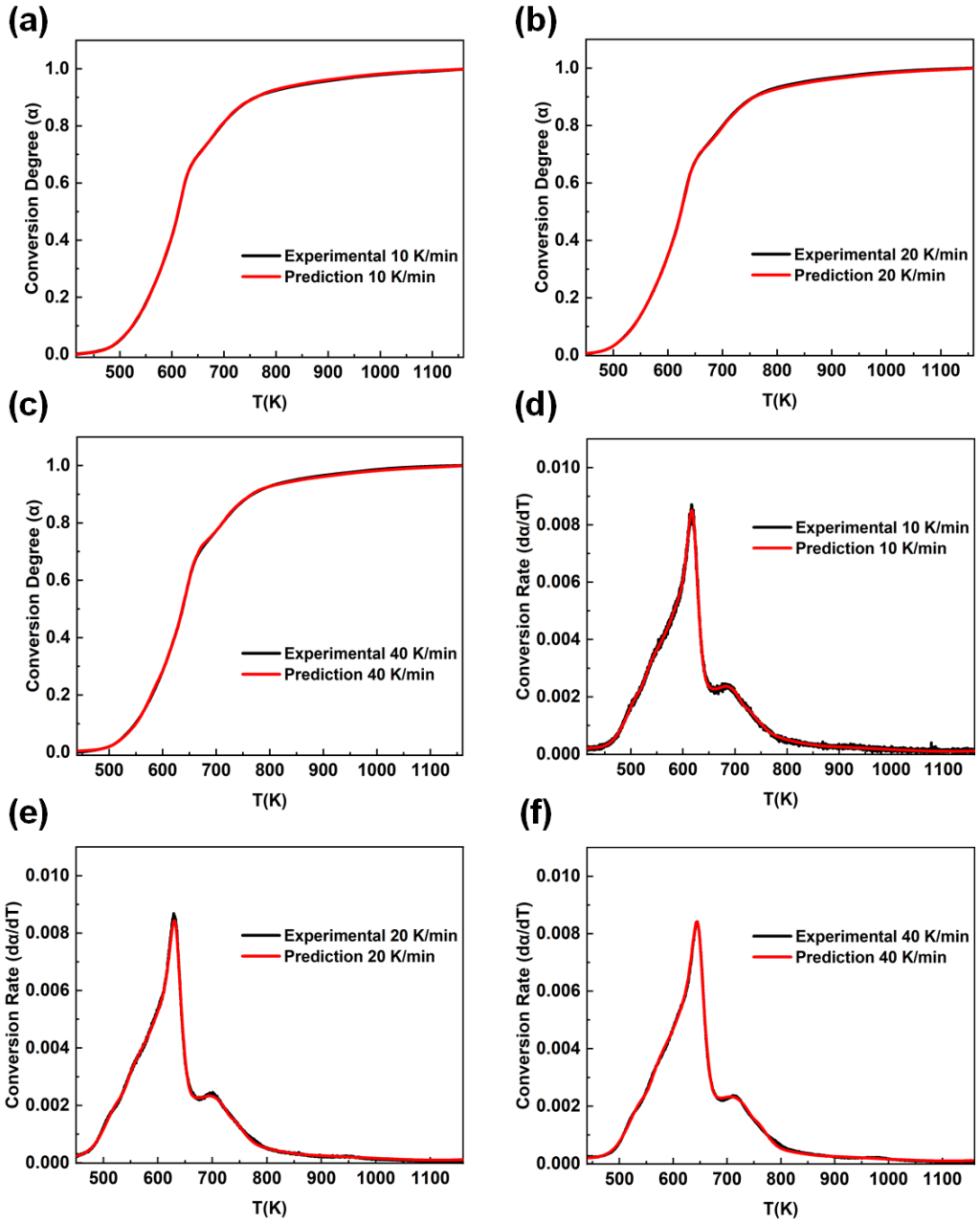

Fig. 5 (a-f). α and $\frac{\mathrm{d}\alpha}{\mathrm{d}T}$ predictions from Coupled Kinetic-ANN Model

Table 4 presents the R^2 and SEP for the conversion degree (α) and conversion rate ($d\alpha/dT$). The R^2 values for the conversion degree (α) were all above 0.9999, while those for $d\alpha/dT$ were above 0.999. The SEP for the conversion degree (α) was below 0.25%, and for $d\alpha/dT$, it was below 0.45%, particularly in the untrained range (40 K/min), where the performance significantly exceeded that of a single model. This indicates that the coupled model performed well across the temperature range, offering substantial predictive advantages. However, at 40 K/min, there was a slight increase in the SEP, but it remained within acceptable limits. This could be attributed to unknown factors affecting the predictions of the coupled model in this range or insufficient training data. Nonetheless, the coupled model demonstrated high accuracy and robustness, significantly outperforming a single model in prediction.

Table 4. R^2 and SEP from the Coupled Kinetic-ANN Model

Heating Rate (K/min)	Conversion Degree ($\boldsymbol{\alpha}$)		Conversion Rate ($\frac{\mathbf{d\alpha}}{\mathbf{dT}}$)	
	R^2	SEP (%)	R^2	SEP (%)
10	0.99997	0.205	0.99961	0.402
20	0.99993	0.227	0.99959	0.407
40	0.99993	0.249	0.99944	0.447

Accuracy of Kinetic, GA-BP-ANN and Coupled Kinetic-ANN Models

This section compares the predictive effectiveness of the kinetic model, the GA-BP-ANN model, and the coupled model (Fig. 6). Figure 6 (a-c) compares the prediction results of the conversion degree for three different heating rates among the three models with the experimental results. Figure 6 (d-f) compares the prediction results of the conversion rate for three different heating rates among the three models with the experimental results. The prediction curves of the coupled model were the most consistent with the experimental curves, followed by GA-BP-ANN, with the kinetic model performing the worst. Figure 7(a) compares the predictive effectiveness of the three models for conversion degree based on R^2 values. Although the kinetic model's predictions were poor, its results were still higher than 0.98. The other models performed well in predicting conversion degree, with R^2 values above 0.99. In particular, the coupled kinetic-ANN model had an R^2 value of more than 0.9999, which was better than both the kinetic model and the GA-BP-ANN model. However, Fig. 7(b) shows that the kinetic model performed extremely poorly in predicting conversion rate ($d\alpha/dT$) at the untrained heating rate of 40 K/min (R^2: 0.74119), whereas the coupled model maintained a high level of accuracy with an R^2 value of 0.99944. However, whether in the trained or untrained regions, it was found that the R^2 value of the conversion degree was consistently higher than that of the conversion rate. This difference may be due to the fact that the conversion rate is derived from the derivative of the conversion degree, making it more susceptible to noise.

Figure 7 (a, c) compares the predictive effectiveness of three models for conversion degree based on R^2 and SEP. Although the kinetic model's predictions were poor, the R^2 results were still higher than 0.98. The other models performed excellently in predicting the conversion degree, with R^2 values above 0.99. In particular, the coupled kinetic-ANN model achieved an R^2 value of more than 0.9999, outperforming both the kinetic model and the GA-BP-ANN model. This is consistent with the SEP trend, which was below 0.25% for the coupled model, compensating for the lack of predictive power of a single model in untrained regions.

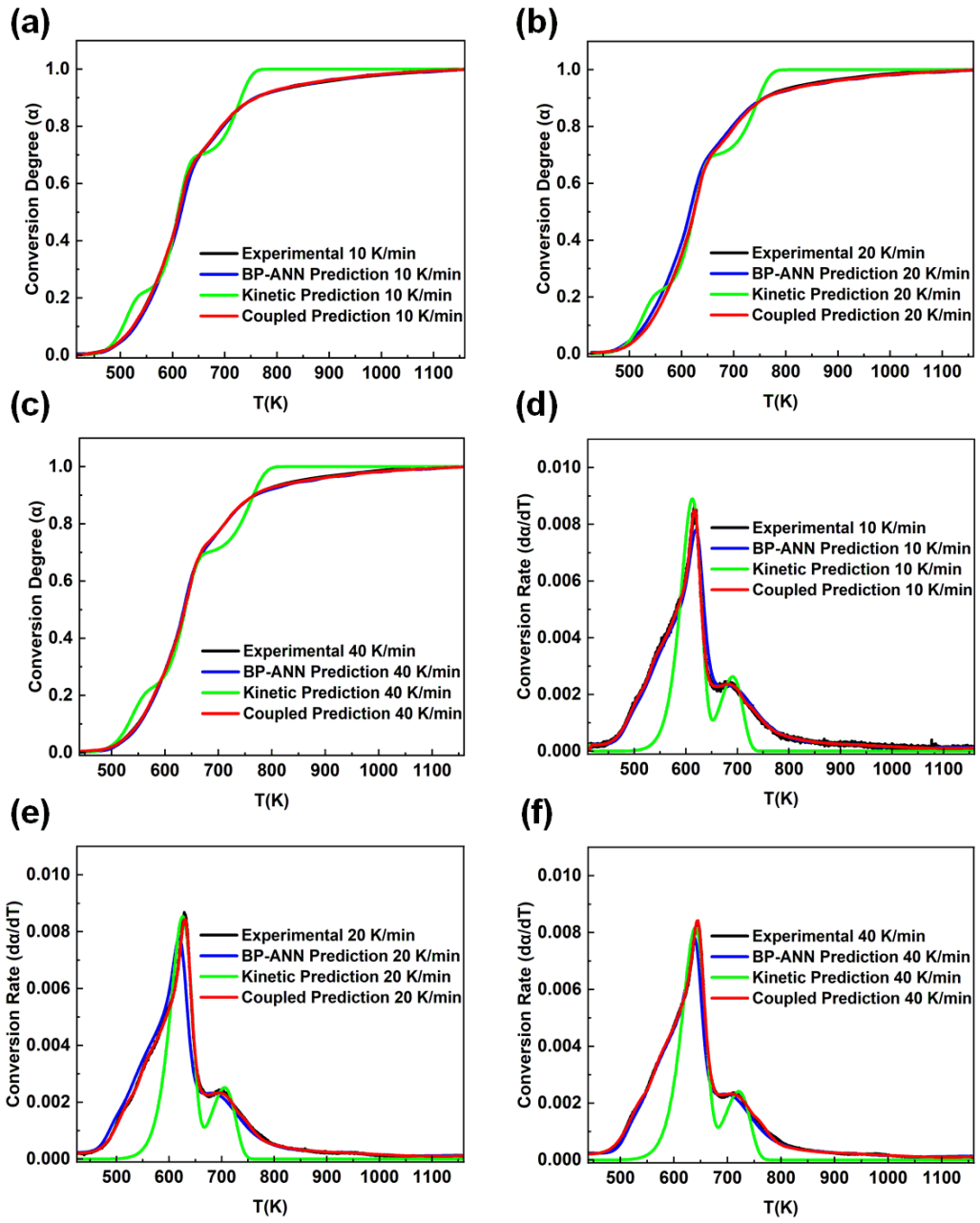

Fig. 6 (a-f). Comparison of $\boldsymbol{\alpha}$ and $\frac{\mathbf{d}\boldsymbol{\alpha}}{\mathbf{d}\boldsymbol{T}}$ predictions at 10, 20 and 40 K/min from three models

However, Fig. 7(b, d) shows that the kinetic model performed extremely poorly in predicting conversion rate ($d\alpha/dT$) at the untrained heating rate of 40 K/min (R^2: 0.74119, SEP: 9.409%). In contrast, the coupled model maintained a high level of accuracy, with an R^2 value of 0.99944 and an SEP value of 0.447%. It was found that the R^2 value of the conversion degree was consistently higher than that of the conversion rate, whether in trained or untrained regions. This difference may be due to the fact that the conversion rate is derived from the derivative of the conversion degree, making it more susceptible to noise.

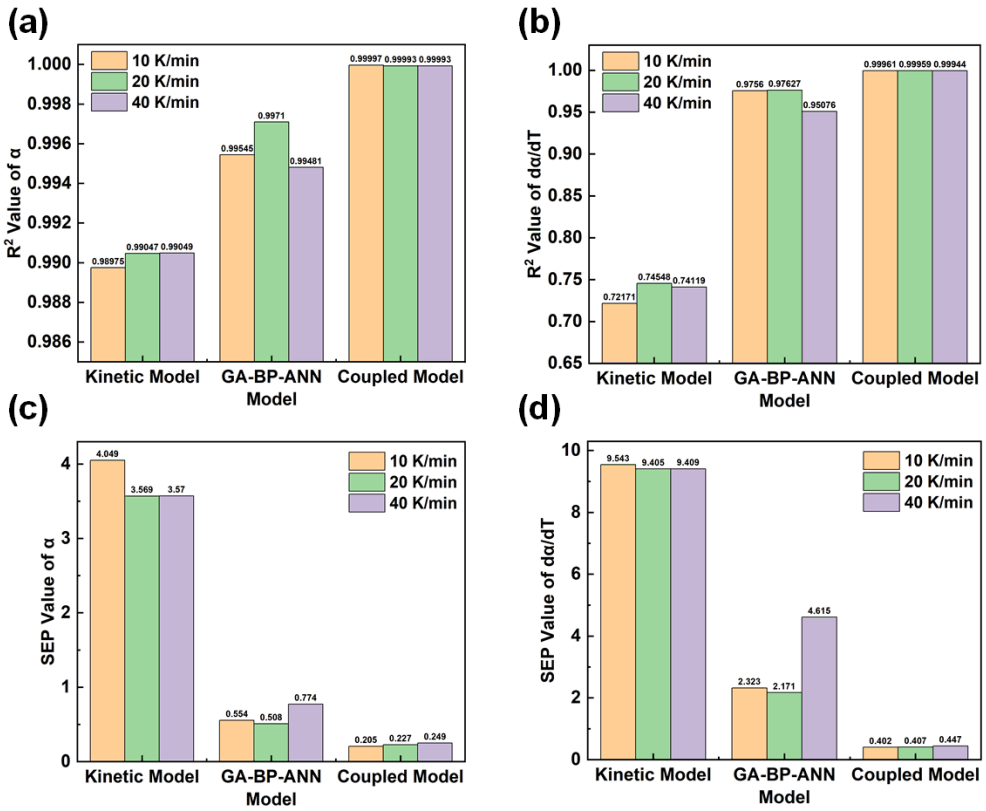

Fig. 7 (a-d). R^2 and SEP comparison of $\boldsymbol{\alpha}$ and $\frac{\mathbf{d}\boldsymbol{\alpha}}{\mathbf{d}\boldsymbol{T}}$ predictions at 10, 20 and 40 K/min from three Models

CONCLUSIONS

1. This paper successfully proposed an innovative biomass pyrolysis modeling scheme that integrates a kinetic model based on chemical reaction mechanisms with an empirically-based machine learning model. When validated against experimental data, the method demonstrated extremely high prediction accuracy, particularly in unfamiliar scenarios, showcasing significant advantages.
2. In the study of chemical reaction kinetic modeling, the introduction of the improved dung beetle optimization algorithm significantly enhances the capability to fine-tune kinetic parameters. This enhancement allows the model to more accurately describe complex pyrolysis processes and improves prediction reliability.
3. Through comparison, it was found that among the three prediction models, predicting the degree of conversion performs better than predicting the conversion rate. This may be due to noise errors in the derivative calculation of conversion rate parameters.

ACKNOWLEDGMENTS

This study is supported by International Science and Technology Cooperation Project of Henan Province (232102521011); Natural Science Foundation of Sichuan

Province (2023NSFSC1253); Regional Innovation Cooperation Project of Sichuan Province (2024YFHZ0148); Agricultural Science and Technology Innovation Project of Chinese Academy of Agricultural Sciences (CAAS-ASTIP-2016-BIOMA).

REFERENCES CITED

Alaba, P., Popoola, S., Abnisal, F., Lee, C., Ohunakin, O., Adetiba, E., Akanle, M., Patah, M., Atayero, A., and Daud, W. (2019). "Thermal decomposition of rice husk: a comprehensive artificial intelligence predictive model," *Journal of Thermal Analysis and Calorimetry* 140, 1811-1823. DOI: 10.1007/s10973-019-08915-0

Breiman, L. (1996). "Mach Learn 24," in: *Stacked Regressions*, 49-64. DOI: 10. 1007/bf00117832

Bi, H., Wang, C., Jiang, X., Jiang, C., Bao, L., and Lin, Q. (2021). "Thermodynamics, kinetics, gas emissions and artificial neural network modeling of co-pyrolysis of sewage sludge and peanut shell," *Fuel* 284, article 118988. DOI: 10.1016/j. fuel. 2020. 118988

Chang, D., Zhang, X., and Zheng, C. (2008). "A genetic algorithm with gene rearrangement for K-means clustering," *Pattern Recognition* 42(7), 1210-1222. DOI: 10. 1016/j. patcog. 2008. 11. 006

Cheng, P., Wang, D., Zhou, J., Zuo, S., and Zhang, P. (2022). "Comparison of the warm deformation constitutive model of GH4169 alloy based on neural network and the Arrhenius model," *Metals* 12(9), article 1429. DOI: 10.3390/met12091429

Conn, A., Gould, N., and Toint, P. (1991). "A globally convergent augmented Lagrangian algorithm for optimization with general constraints and simple bounds," *SIAM Journal on Numerical Analysis* 28, 545-572. DOI: 10.1137/0728030

Ding, Y., Zhang, W., Yu, L., and Lu, K. (2019). "The accuracy and efficiency of GA and PSO optimization schemes on estimating reaction kinetic parameters of biomass pyrolysis," *Energy* 176, 582-588. DOI: 10.1016/j.energy.2019.04.030

Ding, Y., Huang, B., Li, K., Du, W., Lu, K., and Zhang, Y. (2020). "Thermal interaction analysis of isolated hemicellulose and cellulose by kinetic parameters during biomass pyrolysis," *Energy* 195, article 117010. DOI: 10.1016/j.energy.2020.117010

Ding, Y., Jiang, G., Fukumoto, K., Zhao, M., Zhang, X., Wang, C., and Li, C. (2023). "Experimental and numerical simulation of multi-component combustion of typical no-charring material," *Energy* 262 (PB), article 125555. DOI: 10.1016/j.energy.2022.125555

Dubdub, I., and Al-Yaari, M. (2020). "Pyrolysis of low density polyethylene: Kinetic study using TGA data and ANN prediction," *Polymers* 12(4), 891-891. DOI: 10.3390/polym12040891

Dubdub, I., and AlYaari, M. (2021). "Pyrolysis of mixed plastic waste: II. Artificial neural networks prediction and sensitivity analysis," *Applied Sciences* 11(18), 8456. DOI: 10.3390/app11188456

Gbolahan, I., Pobitra, H., Chinyere, C., Ken, C., Abhishek, S., Jorge, P., and Kalpit, S. (2022). "Advances in biosolids pyrolysis: Roles of pre-treatments, catalysts, and co-feeding on products distribution and high-value chemical production," *Journal of Analytical and Applied Pyrolysis* 166, article 105608. DOI: 10.1016/j.jaap.2022.105608

Guo, X., Qin, X., Zhang, Qing., Zhang, Y., Wang, P., and Fan, Z. (2023). "Speaker

recognition based on dung beetle optimized CNN," *Applied Sciences* 13(17), article 9787. DOI: 10.3390/app13179787

Huang, R., Huang, Z., Ran, Y., Xiong, X., Luo, T., Long, E., Mei, Z., and Wang, J. (2021). "Experimental and simulation study on the surface contact between biogas fermentation liquid and straw material based on hydraulic mixing," *Energy* 222, article 111992. DOI: 10.1016/j.energy.2021.119992

Hu, Z., Yuan, Y., Li, X., Tu, Z., Dacres, O., Zhu, Y., Shi, L., Hu, H., Liu, H., Luo, G., and Yao, H. (2022). "Yield prediction of 'Thermal-dissolution based carbon enrichment' treatment on biomass wastes through coupled model of artificial neural network and AdaBoost," *Bioresource Technology* 343, article 126083. DOI: 10.1016/j.biortech.2021.126083

Kersten, S., Wang, X., Prins, W., and van, Swaaij, W. P. M. (2005). "Biomass pyrolysis in a fluidized bed reactor. Part 1: Literature review and model simulations," *Industrial & Engineering Chemistry Research* 23, 8773-8785. DOI: 10.1021/ie0504856

Ka, L., Adetoyese, O., and Chi, W. (2012). "Experimental and modelling studies of biomass pyrolysis," *Chinese Journal of Chemical Engineering* 3, 543-550. DOI: 10.1016/s1004-9541(11)60217-6

Kaczor, Z., Buliński, Z., and Werle, S. (2020). "Modelling approaches to waste biomass pyrolysis: A review," *Renewable Energy* 159, 427-443. DOI: 10.1016/j.renene.2020.05.110

Ke, L., Wu, Q., Zhou, N., Xiong, J., Yang, Q., Zhang, L., Wang, Y., Dai, L., Zou, R., Liu, Y., Ruan, R., and Wang, Y. (2022). "Lignocellulosic biomass pyrolysis for aromatic hydrocarbons production: Pre and in-process enhancement methods," *Renewable and Sustainable Energy Reviews* 165, article 112607. DOI: 10.1016/j.rser.2022.112607

Liborio, O., Arias, S., Mumbach, D., Alves, J., Silva, J., and Pacheco, J. (2024). "Evaluating black wattle bark industrial residue as a new feedstock for bioenergy *via* pyrolysis and multicomponent kinetic modeling," *Renewable Energy* 228, article 120693. DOI: 10.1016/j.renene.2024.120693

Machmudah, S., Wicaksono, D., Happy, M., Winardi, S. Wahyudiono., Kanda, H., and Goto, M. (2020). "Water removal from wood biomass by liquefied dimethyl ether for enhancing heating value," *Energy Reports* 6, 824-831. DOI: 10.1016/j.egyr.2020.04.006

Marchese, L., Kühl, K., Silva, J., Mumbach, G., Alves, R., Alves, J., and Domenico, M. (2024). "Exploring bioenergy prospects from malt bagasse: Insights through pyrolysis with multi-component kinetic analysis and thermodynamic parameter estimation," *Renewable Energy* 226, article 120453. DOI: 10.1016/j.renene.2024.120453

Martín-Lara, M., Blázquez, G., Ronda, A., and Calero, M. (2016). "Kinetic study of the pyrolysis of pinecone shell through non-isothermal thermogravimetry: Effect of heavy metals incorporated by biosorption," *Renewable Energy* 96, 613-624. DOI: 10.1016/j.renene.2016.05.026

Naqvi, R., Tariq, R., Hameed, Z., Ali, I., Taqvi, S., Naqvi, M., Niazi, M., Noor, T., and Farooq, W. (2018). "Pyrolysis of high-ash sewage sludge: Thermo-kinetic study using TGA and artificial neural networks," *Fuel* 233, 529-538. DOI: 10.1016/j.fuel.2018.06.089

Quan, G., Wang, T., Li, Y., Zhan, Z., and Xia, Y. (2016). "Artificial neural network modeling to evaluate the dynamic flow stress of 7050 aluminum alloy," *Journal of*

Materials Engineering and Performance 25, 553-564. DOI: 10.1007/s11665-016-1884-z

Ragauskas, A. J., Williams, C. K., Davison, B. H., Britovsek, G., Cairney, J., Eckert, C. A., Frederick, Jr., W. J., Hallett, J. P., Leak, D. J., Liotta, C. L., *et al*. (2006). "The path forward for biofuels and biomaterials," *Science* 311, 484-489. DOI: 10.1126/science.1114736

Shen, Q., Zhang, D., Xie, M., and He, Q. (2023). "Multi-Strategy enhanced dung beetle optimizer and its application in three-dimensional UAV path planning," *Symmetry* 15(7), article 1432. DOI: 10.3390/sym15071432

Sunphorka, S., Chalermsinsuwan, B., and Piumsomboon, P. (2017). "Artificial neural network model for the prediction of kinetic parameters of biomass pyrolysis from its constituents," *Fuel* 193, 142-158. DOI: 10.1016/j.fuel.2016.12.046

Vo, T., Tran, Q., Ly, H., Kwon, B., Hwang, H., Kim, J., and Kim, S. (2022). "Co-pyrolysis of lignocellulosic biomass and plastics: A comprehensive study on pyrolysis kinetics and characteristics," *Journal of Analytical and Applied Pyrolysis* 163, article 105464. DOI: 10.1016/j.jaap.2022.105464

White, E., Catallo, J., and Legendre, L. (2011). "Biomass pyrolysis kinetics: A comparative critical review with relevant agricultural residue case studies," *Journal of Analytical and Applied Pyrolysis* 91(1), 1-33. DOI: 10.1016/j.jaap.2011.01.004

Wei, H., Xing, J., Luo, K., Peng, Y., Fan, J., Zhang, K., and Wang, H. (2023). "Predicting tobacco pyrolysis based on chemical constituents and heating conditions using machine learning approaches," *Fuel* 335, article 126895. DOI: 10.1016/j.fuel.2022.126895

Xing, J., Luo, K., Wang, H., Gao, Z., and Fan, J. (2019). "A comprehensive study on estimating higher heating value of biomass from proximate and ultimate analysis with machine learning approaches," *Energy* 188, article 116077. DOI: 10.1016/j.energy.2019.116077

Xue, J., and Shen, B. (2022). "Dung beetle optimizer: A new meta-heuristic algorithm for global optimization," *The Journal of Supercomputing* 79, 7305-7336. DOI: 10. 1007/s11227-022-04959-6

Xu, L., Zhou, J., Ni, J., Li, Y., Long, Y., and Huang, R. (2020). "Investigating the pyrolysis kinetics of Pinus sylvestris using thermogravimetric analysis," *BioResources* 15(3), 5577-5592. DOI: 10.15376/biores.15.3.5577-5592

Xu, L., Zhang, Y., Wang, Z., Guo, S., Hao, Y., Gao, Y., Xin, M., Ran, Y., Li, S., Ji, R., Li, H., Jiang, H., He, Q., and Huang, R. (2023). "Kinetic analysis and pyrolysis behavior of pine needles by TG-FTIR and Py-GC/MS," *BioResources* 18(3), 6412-6429. DOI: 10.15376/biores.18.3.6412-6429

Yang, K., Wu, K., and Zhang, H. (2022). "Machine learning prediction of the yield and oxygen content of bio-oil via biomass characteristics and pyrolysis conditions," *Energy* 254, article 124320. DOI: 10. 1016/j. energy. 2022. 124320

Zhang, T., Cao, D., Feng, X., Zhu, J., Lu, X., Mu, L., and Qian, H. (2022). "Machine learning prediction of bio-oil characteristics quantitatively relating to biomass compositions and pyrolysis conditions," *Fuel* 312, article 122812. DOI: 10.1016/j.fuel.2021.122812

Zha, Z., Ge, Z., Ma, Y., Zeng, M., Tao, Y., and Zhang, H. (2022). "Reactivity and kinetics of furfural residue air gasification based on-line gas releasing behaviors in a bubbling fluidized bed," *Combustion and Flame* 237, article 111837. DOI: 10.1016/j.combustflame.2021.111871

Zhong, Y., Ding, Y., Jiang, G., Lu, K., and Li, C. (2023). "Comparison of artificial neural networks and kinetic inverse modeling to predict biomass pyrolysis behavior," *Journal of Analytical and Applied Pyrolysis* 169, article 105802. DOI: 10. 1016/j. jaap. 2022. 105802

Zhu, Y., Cao, Y., Liu, C., Luo, R., Li, N., Shu, G., and Liu, Q. (2020). "Dynamic behavior and modified artificial neural network model for predicting flow stress during hot deformation of Alloy 925," *Materials Today Communications* 25, article 101329. DOI: 10. 1016/j. mtcomm. 2020. 101329

Zhu, H., Dong, Z., Yu, X., Cunningham, G., Umashanker, J., Zhang, X., and Cai, J. (2021). "A predictive PBM-DEAM model for lignocellulosic biomass pyrolysis," *Journal of Analytical and Applied Pyrolysis* 157, article 105231. DOI: 10.1016/j.jaap.2021.105231

Zhu, F., Li, G., Tang, H., Li, Y., Lv, X., and Wang, Xi. (2024). "Dung beetle optimization algorithm based on quantum computing and multi-strategy fusion for solving engineering problems," *Expert Systems with Applications* 236, article 121219. DOI: 10.1016/j.eswa.2023.121219

Article submitted: July 9, 2024; Peer review completed: August 1, 2024; Revised version received: August 9, 2024; Accepted: August 11, 2024; Published: August 26, 2024.
DOI: 10.15376/biores.19.4.7513-7529